

Synthesis of Tubular Graphite Cones through a Catalytically Thermal Reduction Route

Zhenyu Sun, Zhimin Liu,* Jimin Du, Yong Wang, Buxing Han,* and Tiancheng Mu

Center for Molecular Science, Institute of Chemistry, The Chinese Academy of Sciences, Beijing 100080, China

Received: April 6, 2004

This paper describes a catalytically thermal reduction route for the synthesis of tubular graphite cones (TGCs) from the reaction between a mixture of poly(ethylene glycol) and ethylene glycol and magnesium over Fe catalyst decomposed from ferrocene at 640 °C. The base of the cones is in the micrometer scale, tapering gradually to form nanometer-sized tips. The hollow cones, which have a shell made up of cylindrical graphite sheets, have been observed by high-resolution transmission electron microscopy (HRTEM), and some Y-junction TGCs were also observed.

Introduction

Due to their unique structural, mechanical, and electronic properties and consequently their potential applications in many fields, the carbon-based nanomaterials with highly curved graphitic structures have attracted great interest. Since Iijima discovered carbon nanotubes in the arc-discharge apparatus in 1991,¹ a number of novel one-dimensional nanostructures have been reported, including helix-shaped graphitic nanotubes,² graphitic nanocones,³ nanohorns,⁴ conical crystals,^{5,6} microtrees,⁷ carbon onions,⁸ carbon nanoflasks, and large carbon nanocontainers.^{9,10} Recently, Zhang et al.¹¹ synthesized another new carbon nanostructure termed “tubular graphite cones” (TGCs) using a microwave plasma assisted chemical vapor deposition (MPCVD) system with N₂ and CH₄ as the reaction gas and iron needles as substrates. Adopting the MPCVD route with CH₄/H₂ as the reactants and platinum wires as substrates, Mani et al.¹² synthesized carbon nanopipettes with uniform hollowness throughout the length of the structure resembling to the above TGCs. Using a film of gallium covered with molybdenum powder exposed to 18% CH₄/H₂ plasma, Bhimarasetti et al.¹³ synthesized tapered and multijunctioned carbon tubular structures with varying conical angles from 7° to 58° controlled via the gas-phase chemistry. The new morphologies exhibit thin walls (10–30 nm) and very large internal diameters (up to 2.5 μm).

The tubular cones have potential use as tips for scanning probe microscopy,^{11,14} with greater rigidity and easier mounting than presently used carbon nanotubes. Their morphology and structure also suggests such potential applications as electron emitters,¹⁵ nozzles for nanojets (after the tip removal),¹⁶ and so on. Herein we report a novel route for the fabrication of another type of TGCs, which have uniform wall thickness. In this method, poly(ethylene glycol) and ethylene glycol are used as the carbon source, and magnesium and ferrocene are used as the reductant and catalyst, respectively. The TGCs were prepared by a catalytically thermal reduction process. In comparison with the MPCVD, the adopted method is more facile.

Experimental Section

Synthesis of TGCs. In a typical experiment, 8 g of poly(ethylene glycol) (PEG 800) was first dissolved in 6.3 g of

ethylene glycol to form a homogeneous solution, and then 0.72 g of magnesium and 0.18 g of ferrocene were added. The above reactants were all placed into a 25 mL stainless steel autoclave. The autoclave was sealed and kept at 640 °C for 5 h, and then it was cooled to room temperature naturally. The dark precipitate in the autoclave was collected and sequentially washed with absolute ethanol, dilute HCl aqueous solution, and distilled water. The final product was dried under vacuum at 70 °C for 6 h. The yield of TGCs, estimated from scanning electron microscopy (SEM) observation, is about 40%.

Characterization Techniques. The purity and phase structure of the products were obtained by X-ray powder diffraction (XRD) analysis, which was performed on a Rigaku D/MAX-RC X-ray diffractometer with Cu K α radiation. The morphologies of the samples were observed through scanning electron microscopy (SEM) and transmission electron microscopy (TEM), which were made on a JEOL JSM-6700F field emission microscope and on a JEOL 2010 transmission electron microscope, using an accelerating voltage of 200 kV, respectively. The microstructure of TGCs was studied by high-resolution transmission electron microscopy (HRTEM) observation, which was operated with a Hitachi-9000 NAR electron microscope, using an accelerating voltage of 300 kV.

Information about the vibrational properties of the carbon material was obtained by Raman spectroscopy. The Raman spectrum was recorded at ambient temperature on a RM 2000 Raman spectrometer with an argon ion laser at an excitation wavelength of 514.5 nm.

Results and Discussion

A typical XRD pattern of the as-prepared products is shown in Figure 1, which demonstrates that graphite is the dominant feature. The diffraction peaks at 26.5°, 42.4°, 54.7°, and 77.4° observed in the XRD pattern of the products can be attributed to (002), (100), (004), and (110) reflections of the hexagonal graphite structure, respectively. However, weak diffraction peaks of MgO also can be observed (JCPDS Card Files, No. 77-2364), which suggests that MgO was encapsulated inside the TGCs and was difficult to remove even after long treatment with dilute HCl.

The as-prepared products were detected by means of scanning electron microscopy (SEM), and a typical image is shown in Figure 2A. It can be seen that a large quantity of TGCs with a

* Address correspondence to this author. Z.L.: phone 8610-62562821, fax 8610-62562821, e-mail liuzm@iccas.ac.cn.

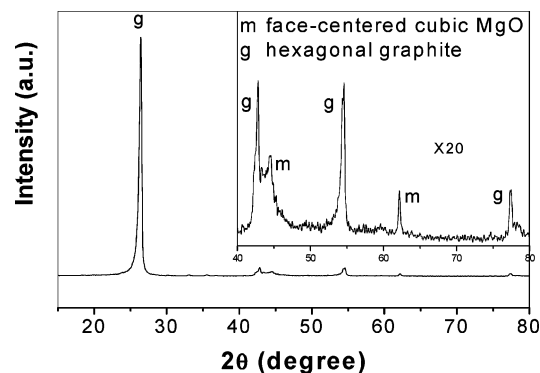


Figure 1. Powder X-ray diffraction patterns of TGCs.

pointed tip was obtained. Panels B, C, and D in Figure 2 show transmission electron microscopy (TEM) images of some TGCs. The TEM observation demonstrates that the average tip apex angle is in the range of 10–20°, the average length of the as-prepared TGCs is about 2.5 μm , and the diameter of the hollow interiors varies from about several nanometers to hundreds of nanometers, but the thickness of their walls remains almost

constant as shown in Figure 2B,C,D, which is different from those values reported in the literature.^{3,6,7,11,12} The electron diffraction (ED) pattern of the walls of the TGCs was collected during TEM observation. The inset in Figure 2C is characteristic with a ring for (002), together with a ring for (100) and a pair of weak arcs for (004) diffractions. The appearance of (002) diffraction as a pair of arcs indicates some orientation of the (002) plane in the TGCs. It also can be observed that some TGCs seem to contain some compounds in their hollow interiors. Energy-dispersive analysis of X-rays (EDAX) for these TGCs during the TEM observation indicates that they are partly filled with MgO, as illustrated in Figure 2E. This is consistent with the XRD results.

In the TEM examination of the as-prepared products, some Y-junction TGCs with no obstructions at the Y-junction point were also observed, as displayed in Figure 2D. Interestingly, the internal diameter of the two coalesced TGCs is found to be almost equivalent, similar to that of the structures reported by Bhimarasetti et al.¹³ The fraction of Y-junction TGCs in the products estimated from the TEM observation is approximately 10%. Complex three-point nanotube junctions have been proposed as the building blocks of nanoelectronics.¹⁷ The size

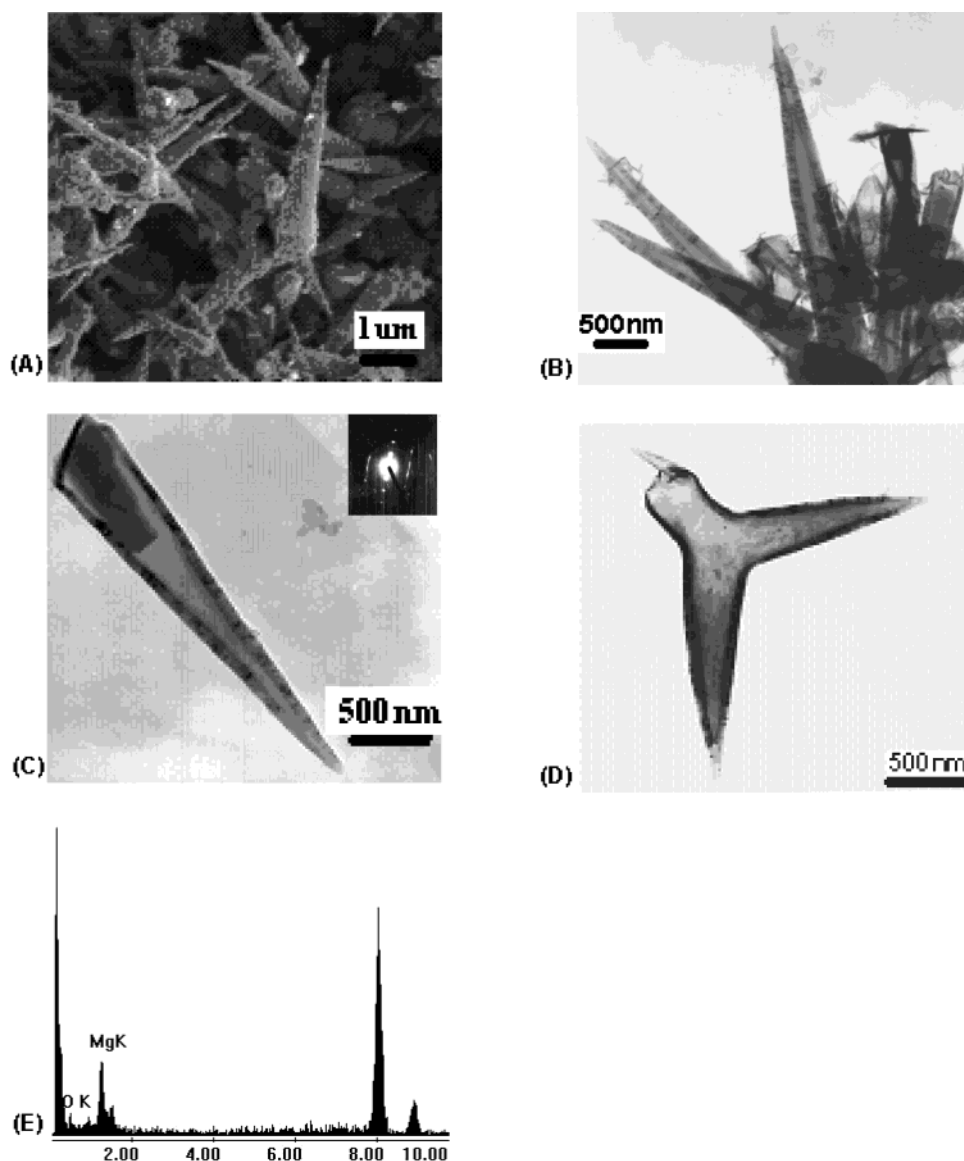


Figure 2. (A) SEM image of TGCs; (B) TEM image of TGCs; (C) TEM image of a typical TGC, the inset is the ED pattern of the walls of TGC; (D) TEM image of a representative of Y-junction TGCs; and (E) EDAX analysis of TGC in (C).

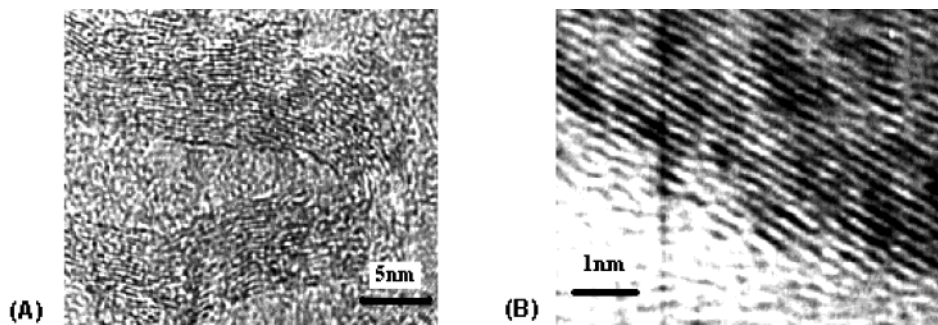


Figure 3. HRTEM images of a TGC: (A) the TGC tip and (B) the wall of the TGC.

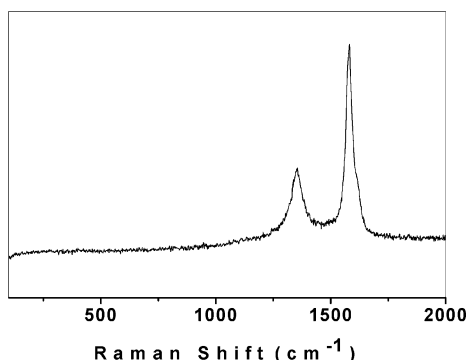


Figure 4. Raman spectrum of as-prepared sample at room temperature.

and microstructure of the Y-junction TGCs also contribute to such promising applications as various microfluidic, micro-reactor, etc.

The detailed microstructures of TGCs were further investigated by HRTEM, and the results are shown in Figure 3. This reveals that the wall layers of the TGCs exhibit well-defined cylindrical morphology with interlayer spacing of about 0.34 nm, which is the same as that of carbon nanotubes.¹⁸

A representative Raman spectrum of the obtained TGCs is illustrated in Figure 4, which shows the typical features similar to those of multiwalled carbon nanotubes,¹ but different from those of graphite polyhedral crystals (GPCs) which have a weak D band and a higher perfection.⁶ The peak at 1581 cm^{-1} (G-band) corresponds to an E_{2g} mode of hexagonal graphite and is related to the vibration of sp^2 -bonded carbon atoms in a 2-dimensional lattice, such as in a graphite layer. The D-band at about 1330 cm^{-1} is associated with vibrations of carbon atoms with dangling bonds in plane terminations of disordered graphite or glassy carbons.

To study the effect of reaction conditions on the formation of TGCs, a series of related experiments were carried out. The results showed that the reaction temperature played a significant role in the production of TGCs. When the temperature was lower than 600 °C, products were dominated by graphite sheets, and TGCs could not be observed by TEM observation.

It is very difficult to give a confirmed growth mechanism of the TGCs. A variety of nucleation and growth models relevant to curved carbon structures have been proposed, among which the “pentagon-road”^{19,20} and the “ring-stacking”²¹ models are the best known. A theoretical study with MD^{22,23} illustrated that pieces of graphite sheets would have many dangling bonds, especially under high temperature. Thus it is difficult to retain the planar morphology of graphite sheets. When rolled into a scroll, graphite sheets can form conical graphite whiskers,²⁴ while the explanation for carbon nanopipettes growth was given on the basis of the selective etching and simultaneous growth modes occurring in the plasma.¹² In another attempt,

the formation of graphite conical crystals (GCCs) was attributed to the nucleation on catalyst particles and growth axially due to a significantly faster longitudinal growth rate in comparison to radial thickening.⁷ Our EDS analysis demonstrated that solid MgO particles were encapsulated in the TGCs. In addition, it is worth noting that MgO has been suggested to be a good support of catalyst for SWNT synthesis.²⁵ In this work, Fe atoms originating from ferrocene act as the catalyst while Mg is the reductant and MgO is produced. On the basis of the discussion above, we propose that carbon produced nucleates at Fe–MgO interface and thus favors the formation of carbon cap around the MgO particles, which is in line with the mechanism presented by Bhimarasetti et al.¹³ While the wall grows upward tangential to the MgO particle shown by the HRTEM image (Figure 2B), the MgO–carbon interface lifts the MgO particle and subsequently gives rise to the TGCs structure with tapering diameter. Y-junctions within TGCs could be associated with the spontaneous coalescence of MgO particles into bigger ones. The growth mechanism of the TGCs still requires further work.

Conclusions

In summary, TGCs have been successfully synthesized by catalytically thermal reduction of poly(ethylene glycol) and ethylene glycol mixture over ferrocene and magnesium powder. We hope this simple method will contribute to the expansion of the scope of the synthesis and promising use of TGCs. Further work is still required to understand the exact formation mechanism of TGCs.

Acknowledgment. This work is financially supported by the National Natural Science Foundation of China (No. 20374057).

References and Notes

- (1) Iijima, S. *Nature* **1991**, 354, 56.
- (2) (a) Amelinckx, S.; Zhang, X. B.; Bernaerts, D.; Zhang, X. F.; Ivanov, V.; Nagy, J. B. *Science* **1994**, 265, 635. (b) Ivanov, V.; Nagy, J. B.; Lambin, P.; Licas, A.; Zhang, X. B.; Zhang, X. F.; Bernaerts, D.; Van Tendeloo, G.; Amelinckx, S.; Van Landuyt, J. *Chem. Phys. Lett.* **1994**, 223, 329.
- (3) Krishnan, A.; Dujardin, E.; Treacy, M. M. J.; Hugdahl, J.; Lynum, S.; Ebbesen, T. W. *Nature* **1997**, 388, 451.
- (4) Murata, K.; Kaneko, K.; Kokai, F.; Takahashi, K.; Yudasaka, M.; Iijima, S. *Chem. Phys. Lett.* **2000**, 331, 14.
- (5) Gogotsi, Y.; Libera, J. A.; Kalashnikov, N.; Yoshimura, M. *Science* **2000**, 290, 317.
- (6) Gogotsi, Y.; Dimovski, S.; Libera, J. A. *Carbon* **2002**, 40, 2263.
- (7) Ajayan, P. M.; Nugent, J. M.; Siegel, R. W.; Wei, B.; Kohler-Redlich, P. *Nature* **2000**, 404, 243.
- (8) Ugarte, D. *Nature* **1992**, 359, 707.
- (9) Liu, S.; Tang, X.; Yin, L.; Koltypin, Y.; Gedanken, A. *J. Mater. Chem.* **2000**, 10, 1271.
- (10) Liu, S.; Boeshore, S.; Fernandez, A.; Sayagues, M. J.; Fischer, J. E.; Gedanken, A. *J. Phys. Chem. B* **2001**, 105, 7606.
- (11) Zhang, G. Y.; Jiang, X.; Wang, E. *Science* **2003**, 300, 18.
- (12) Mani, R. C.; Li, X.; Sunkara, M. K.; Rajan, K. *Nano Lett.* **2003**, 3, 671.

- (13) Bhimarasetti, G.; Sunkara, M. K.; Graham, U. M.; Davis, B. H.; Suh, C.; Rajan, K. *Adv. Mater.* **2003**, *15*, 1629.
- (14) Stavens, K. B.; Andres, R. P. Use of multi-walled carbon nanotubes for conductive probe scanning force microscopy (CP-SFM). In *MRS Symposium 2001*; Materials Research Society, 2001; pp A.8.6.1–A.8.6.6.
- (15) Ren, Z. F.; Huang, Z. P.; Wang, D. Z.; Wen, J. G.; Xu, J. W.; Wang, J. H. *Appl. Phys. Lett.* **1999**, *75*, 1086.
- (16) Moseler, M.; Landman, U. *Science* **2000**, *289*, 1165.
- (17) (a) Menon, M.; Srivastava, D. *Phys. Rev. Lett.* **1997**, *79*, 4453. (b) Menon, M.; Srivastava, D. *J. Mater. Res.* **1998**, *13*, 2357. (c) Fuhrer, M. S.; Nygard, J.; Shih, L.; Forero, M.; Yoon, Y. G.; Mazzone, M. S. C.; Choi, H. J.; Ihm, J.; Louie, S. G.; Zettl, A.; McEuen, P. L. *Science* **2000**, *288*, 494. (d) Li, J.; Papadopoulos, C.; Xu, J. *Nature* **1999**, *402*, 253.
- (18) Saito, Y.; Yoshikawa, T.; Bandow, S.; Tomita, M.; Hayashi, T. *Phys. Rev. B* **1993**, *47*, 1907.
- (19) Zhang, Q. L. *J. Phys. Chem.* **1986**, *90*, 525.
- (20) Smalley, R. E. *Acc. Chem. Res.* **1992**, *25*, 98.
- (21) Wakabayashi, T.; Achiba, Y. *Chem. Phys. Lett.* **1992**, *190*, 465.
- (22) Robertson, D. H.; Brenner, D. W.; White, C. T. *J. Phys. Chem.* **1992**, *96*, 6133.
- (23) Han, S. S.; Lee, K. S.; Lee, H. M. *Chem. Phys. Lett.* **2004**, *383*, 321.
- (24) Bacon, R. *J. Appl. Phys.* **1960**, *31*, 283.
- (25) (a) Colomer, J. F.; Stephan, C.; Lefrant, S.; Tendeloo, G. V.; Willems, I.; Konya, Z.; Fonseca, A.; Laurent, C.; Nagy, J. B. *Chem. Phys. Lett.* **2000**, *317*, 83. (b) Jeong, H. J.; An, K. H.; Lim, S. C.; Park, M. S.; Chang, J. S.; Park, S. E.; Eum, S. J.; Yang, C. W.; Park, C. Y.; Lee, Y. H. *Chem. Phys. Lett.* **2003**, *380*, 263. (c) Liu, B. C.; Lyu, S. C.; Jung, S. I.; Kang, H. K.; Yang, C. W.; Park, J. W.; Park, C. Y.; Lee, C. J. *Chem. Phys. Lett.* **2004**, *383*, 104.